ELSEVIER

Journal of Electroanalytical Chemistry 500 (2001) 533–542

Journal of Electroanalytical Chemistry

www.elsevier.nl/locate/jelechem

Anodisation of copper in thiourea- and formamidine disulphide-containing acid solution. Part I. Identification of products and reaction pathway

A.E. Bolzán, A.S.M.A. Haseeb [1], P.L. Schilardi, R.C.V. Piatti, R.C. Salvarezza, A.J. Arvia *

Instituto de Investigaciones Fisicoquímicas Teóricas y Aplicadas — INIFTA — (U.N.L.P., CONICET, CICBsAs), Sucursal 4, Casilla de Correo 16, 1900 La Plata, Argentina

Received 15 April 2000; received in revised form 15 June 2000; accepted 16 June 2000

Dedicated to Roger Parsons with our gratitude after 37 years serving the electrochemical community as Editor of the Journal of Electroanalytical Chemistry

Abstract

The anodic behaviour of copper in aqueous 0.5 M sulphuric acid containing different amounts of dissolved thiourea or formamidine disulphide was investigated at 298 K, combining data from electrochemical polarisation, chemical analysis, UV–vis spectroscopy, XPS and EDAX analysis, and structural information on copper–thiourea complexes. The main reactions depend on the applied potential and initial thiourea concentration. In the potential range $-0.30 \leq E \leq 0.075$ V (versus SCE), the electro-oxidation of thiourea to formamidine disulphide, the formation of Cu(I)–thiourea soluble complexes, and Cu(I)–thiourea complex polymer-like films, are the most relevant processes. The formation of this film depends on certain critical thiourea/copper ion molar concentration ratios at the reaction interface. At low positive potentials, the former reaction is under intermediate kinetic control, with the diffusion of thiourea from the solution playing a key role. For $E \geq 0.075$ V, soluble Cu(II) ions in the solution are formed and the anodic film is gradually changed to another one consisting of copper sulphide and residual copper. The new film assists the localised electrodissolution of copper. A complex reaction pathway for copper anodisation in these media for the low and high potential range is advanced.

Keywords: Anodic copper dissolution; Thiourea; Corrosion inhibitor

1. Introduction

In spite of a continued interest in thiourea (TU) as a corrosion inhibitor of metals in acid media [1–9], the mechanism of inhibitions is still controversial. It is generally agreed that the extent of corrosion inhibition by TU increases with its concentration (c_{TU}) up to a certain critical value beyond which the inhibition effect decreases. However, values of the TU critical concentration ($c_{TU,c}$) reported in the literature vary widely. It is generally held that TU inhibits corrosion by blocking surface sites through adsorption. The initial increase in inhibition efficiency is suggested to be due to increased surface coverage by a molecular form of TU [3]. The reason for the decrease in inhibition efficiency above $c_{TU,c}$ is still a matter of discussion. Accordingly, with increasing concentration of TU in the bulk solution, the interfacial concentration of protonated TU increases and leads to a decrease in inhibition efficiency. It has already been proposed [4] that protonation of TU seems to be the reason for the decrease in efficiency.

Thiourea can slowly reduce Cu(II) ions to form $[Cu(TU)_n]^+$ $(n = 1, 2, 3, 4)$ complex species of known stability [10–12], and formamidine disulphide (FDS). A previous study [13] concluded that Cu(I) forms a soluble stable ionic complex with excess of TU, described as

* Corresponding author. Tel.: +54-221-425-7430; fax: +54-221-425-4642.

E-mail address: ajarvia@inifta.unlp.edu.ar (A.J. Arvia).

[1] On leave from Bangladesh University of Engineering and Technology, Dhaka, Bangladesh.

0022-0728/01/$ - see front matter
PII: S0022-0728(00)00217-5

$[Cu(TU)]^+$, which is characterised by an absorption band at 240 nm [11]. The redox couple TU/FDS formed in the presence of Cu(II) ions exhibits a coherent polarographic anodic–cathodic wave near 0.242 V (SCE) [14].

For $c_{TU} < 1$ mM, weak copper–TU interactions are dominant, whereas for $c_{TU} > 1$ mM strong effects are observed, leading most likely to 1:1 complexes when there is a considerable excess of Cu(II) ions with respect to TU [15]. It has been reported that, seemingly, at low c_{TU}, the complex formed would be $CuSCNH_2(=NH)$ and, at high c_{TU}, $[Cu(TU)]^+$ [15].

Thiourea undergoes condensation to polythiourets, as concluded from the linear increase in polymer concentration with time and the reversibility of polymerisation [16]. The insoluble product formed from the chemical reaction of Cu(I) and TU has been described as a salt of a $[Cu_xTU_y]^{x+}$ complex cation, with $x < y$. These salts are known to occur for anions such as ClO_4^- [17], NO_3^- [18], Cl^- [19] and either HSO_4^- or SO_4^{-2} [20].

Recently [21], complex salts of Cu(I)–TU such as $[Cu_2(TU)_5]^{2+}$ (complex **I**), $[Cu_4(TU)_7]^{4+}$ (complex **II**) and $[Cu_2(TU)_6]^{2+}$ (complex **III**) have been crystallised from aqueous solutions. The structure and composition of these sulphate salts were determined by X-ray diffractometry [21]. These salts were obtained from either the anodisation of copper in TU-containing 0.5 M sulphuric acid solutions or simply by mixing different amounts of dissolved TU and aqueous acid copper sulphate. It appears that the formation of Cu(I)–TU complex structures was determined mainly by the ionic copper molar ration at the reaction interface. Complexes **I** and **III** are soluble and easy to recrystallise from solutions having a Cu(I):TU molar ratio lower than 4:7. Insoluble complex **II** is formed as a polymer-like solid for a Cu(II):TU molar ratio close to 4:7. Evidence of the formation of a copper–TU–sulphate complex film in the potential range related to copper electrodissolution has been gathered from electrochemical experiments using a quartz crystal microbalance [22].

In this paper we describe the complexity of the anodic electro-oxidation of copper in both TU- and FDS-containing aqueous sulphuric acid solutions at 298 K by combining electrochemical experiments, UV–vis spectroscopy, and chemical, XPS and EDAX analysis. At low potentials ($-0.30 \le E \le 0.07$ V) and $c_{TU} < c_{TU,c} \approx 2.5$ mM, the electro-oxidation of TU to FDS and the copper electrodissolution as Cu(I), are the most relevant processes yielding soluble ionic complex species. The same products are formed from the electrodissolution of copper in FDS-containing solutions. These reactions take place on a copper surface mostly covered by TU. For $c_{TU} > c_{TU,c}$, a passivating film consisting of an insoluble Cu(I)–TU complex is formed. The faradaic yield and nature of both the soluble products and the insoluble passivating film depend on the applied potential and TU:ionic copper molar concentration ratio at the reaction interface. At high potentials (> 0.07 V), when the passivity breakdown potential is exceeded, the electrodissolution of copper as Cu(II) occurs. This reaction takes place in the presence of a heterogeneous film resulting from the electrochemical oxidation of TU and FDS-derivatives anodically produced at the copper electrode. The reaction pathway of copper electrodissolution in TU-containing aqueous sulphuric acid, in both the low and the high potential range, is discussed combining experimental data and structural information on copper–TU complexes that have been produced both from a chemical reaction in solution, and copper anodisation in aqueous TU + copper-containing sulphuric acid [21,23]. The kinetics of anodic film growth followed by SEM and in situ transversal imaging observations are presented in Part II [24]. The two parts of the paper are closely intertwined. They provide a unifying overview of the complex copper–TU and copper–FDS systems taking into account the chemical and electrochemical aspects of these systems. A number of conclusions derived from data resulting from different techniques, as well as proposals that may stimulate new research in the field, are presented.

2. Experimental

Polarisation measurements were carried out in a conventional three-electrode glass cell. A platinum sheet and a saturated calomel electrode (SCE) were used as counter and reference electrodes, respectively. Working electrodes were made from electrorefined copper wire (diameter 0.5 mm and exposed length 13 mm). Each working electrode was electropolished in concentrated phosphoric acid prior to starting the polarisation runs [25]. For comparison, a couple of experiments were also run using a working electrode consisting of a platinum strip of the same dimensions as that of the copper working electrode. Ohmic drop correction to the working electrode potential was negligible, i.e. $E \cong \eta_a + \eta_d$ where η_a and η_d denote the activation and mass transport overpotentials, respectively.

A series of TU-containing aqueous sulphuric acid solutions were used. They were prepared by adding TU (Fluka, puriss. p.a.) in concentrations ranging from 0 to 15 mM to the base electrolyte of 0.5 M sulphuric acid (Merck, p.a. and Milli-Q* water). Solutions containing 0.5 mM FDS (ICN, 97%) in the base electrolyte were also utilised. Before each measurement, solutions were deaerated by bubbling nitrogen for about 20 min.

Thallium underpotential deposition (upd) from 0.1 mM thallium sulphate (Merck p.a.) + 0.5 M sulphuric

acid, as a test reaction to study the adsorption of TU on copper at low potentials was also performed.

The electrochemical instrumentation consisted of a PAR model 362 scanning potentiostat coupled to a Houston Omnigraphic recorder. The polarisation curves were recorded at a scan rate of 0.005 V s^{-1} to approach quasi-steady state polarisation conditions.

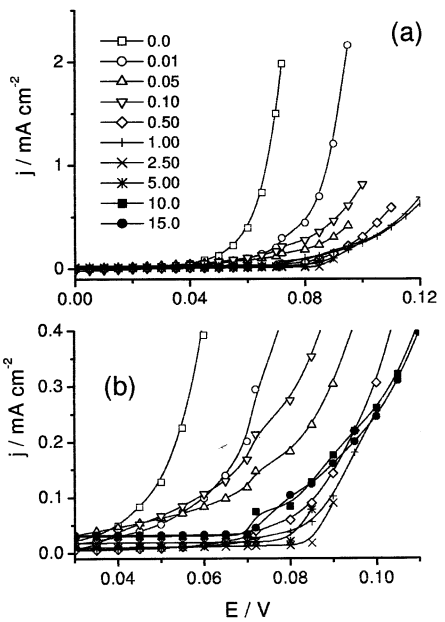

Fig. 1. Copper anode polarisation curves run in $c_{TU} + 0.5$ M sulphuric acid ($0 \le c_{TU} \le 15$ mM) at $v = 0.005$ V s^{-1}. (a) Full curves. (b) Magnified plot of the region of the polarisation curves where inflections are observed. Anode apparent area = 0.2 cm^2. Temperature: 298 K.

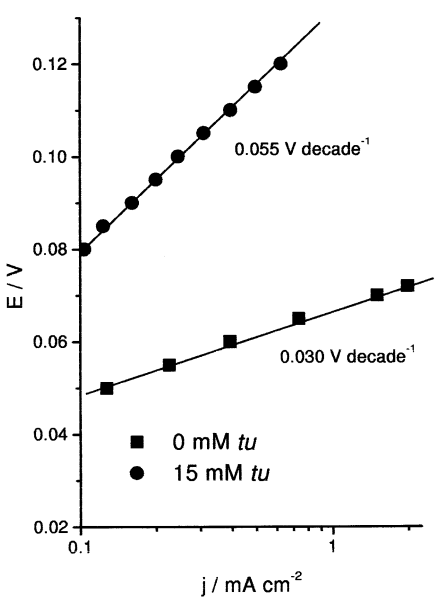

Fig. 2. Tafel plots for the electrodissolution of a copper electrode in 0.5 M sulphuric acid and in 15 mM TU + 0.5 M sulphuric acid. Anode apparent area = 0.2 cm^2. $v = 0.005$ V s^{-1}. Temperature: 298 K.

Samples for XPS and EDAX analysis were prepared at room temperature using an electrorefined copper sheet anode of exposed area 5×7 mm^2. The anode was placed horizontally with its exposed area facing up in order to avoid any mechanical dislodgement of the film. EDAX data were obtained with XL30 FEG Philips equipment. XPS data were obtained using ESCA 3 Mark II equipment with Mg–K_α X-ray ($h\nu = 1253.6$ eV) as the excitation radiation. The binding energies were measured with an accuracy of ± 0.1 eV.

The UV–vis spectra were recorded using a Cary spectrophotometer running absorbance spectra in the range 900 to 190 nm for the detection of copper and TU–copper species in solution.

All the measurements were performed at 298 K.

3. Results

3.1. Polarisation curves

The anodic polarisation curves (Fig. 1) plotted as j versus E, where j is the anodic current density referred to the geometric area of the working electrode, and E is the applied potential referred to the SCE scale, were recorded at 0.005 V s^{-1} in 0.5 sulphuric acid containing different amounts of TU. In the TU-free solution, the polarisation curve fits a Tafel line in the range 0.05–0.07 V with slopes $b_T = \Delta E/\Delta \log j$ in the range $0.030 \le b_T \le 0.040$ V $decade^{-1}$ (Fig. 2), in agreement with earlier reported results [26].

In TU-containing solutions, polarisation curves showed two different types of behaviour, depending on whether $c_{TU} < 0.10$ mM or $c_{TU} > 0.10$ mM. In the former case, positive polarisation increases with c_{TU} as expected for the increase in electrode surface coverage by TU adsorbates. On the other hand, for $c_{TU} > 0.10$ mM, polarisation curves show a passivity range extending from 0.04 to 0.07 V, the passivity current first decreasing to a minimum value for $c_{TU} \approx 2.5$ mM, and then increasing as c_{TU} is increased up to 15 mM.

For $c_{TU} < 0.10$ mM, the first portion of the j versus E curves, i.e. in the range $-0.01 \le E \le 0.07$ V, corresponds to the electro-oxidation of TU to FDS and the simultaneous electrodissolution of copper as soluble Cu(I)–TU complex ions. The rate of these reactions increases almost linearly with c_{TU}. In this range of potentials the increase in the anodic polarisation with c_{TU} can be related to a hindrance of the electrodissolution reaction produced by the gradual increase in copper surface coverage by adsorbates [27,28].

For $c_{TU} > 0.10$ mM, in the potential range $0.04 \le E \le 0.075$ V, passivity is due to the formation of an insoluble Cu(I)–TU complex forming a polymer-like film (hereafter denoted as film I). It should be noted

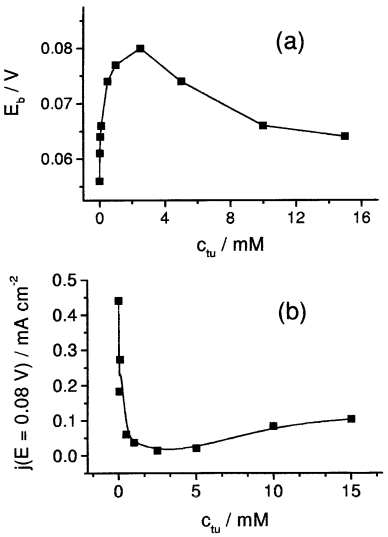

Fig. 3. (a) Dependence of the breakdown potential (E_b) on TU concentration. Copper anode in $c_{TU} + 0.5$ M sulphuric acid ($0 \leq c_{TU} \leq 15$ mM). (b) Dependence of the anodic current density read at $E = 0.08$ V on c_{TU}. Temperature: 298 K.

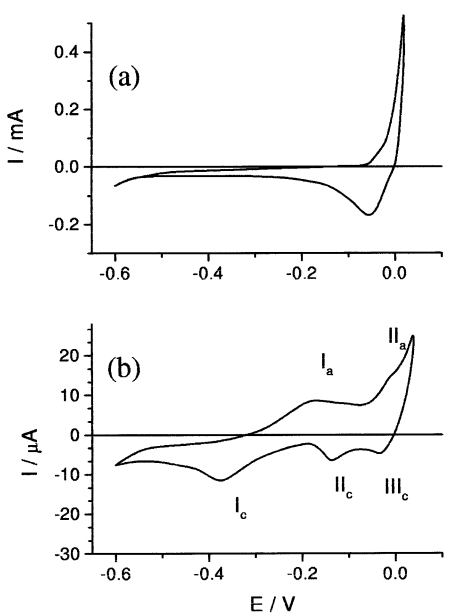

Fig. 4. Cyclic voltammograms of copper anodes in: (a) 0.5 M sulphuric acid (blank); (b) 0.5 mM TU + 0.5 M sulphuric acid. $v = 0.05$ V s^{-1}. Temperature: 298 K.

that the small passivity range related to film I is determined by the potential range where the electro-oxidation of TU to FDS takes place and the threshold potential for copper electrodissolution as the soluble Cu(II) species. Copper electrodissolution across film I then becomes the most relevant process, as described further on. The increase in the passivity current when $c_{TU} > 2.5$ mM suggests that the average thickness ($\langle h \rangle$) of film I diminishes with increasing c_{TU}. This is consistent with the increase in solubility of film I with c_{TU} yielding soluble Cu(I)–TU complexes of different stoichiometries [21].

At $E > 0.07$ V, copper electrodissolution as aqueous Cu(II) ions, and the formation of an insoluble residue containing S, CN and Cu (film II) result from the electrodecomposition of TU and FDS derivatives. Film II behaves as a heterogeneous film that changes the kinetics of the global anodic reaction assisting the localised corrosion of copper [29]. The upper potential limit of the passivity range where the anodic current enhancement is observed decreases from ca. 0.085 V for $c_{TU} = 2.5$ mM to ca. 0.070 V for $c_{TU} = 15$ mM. These potential values approach the threshold potential predicted by thermodynamics for copper electrodissolution as Cu(II) species in 0.5 M sulphuric acid for a copper ion concentration of about 0.001 mM [30]. The breakdown potential (E_b) is preceded by a small current hump that becomes clearer for the range $2.5 \leq c_{TU} \leq 10$ mM. The value of c_{TU} goes through a maximum for $c_{TU} \approx 2.5$ mM (Fig. 3a). The reverse effect can be observed for the same value of c_{TU} by plotting the value of j read at $E = 0.08$ V versus c_{TU} (Fig. 3b). From these plots, the maximum value of E_b is obtained for a critical TU concentration $c_{TU,c} = 2.5$ mM. For $E > E_b$ the polarisation curves for copper electrodissolution as soluble Cu(II) from 0.08 to 0.12 V, fit E versus $\log j$ linear relationships with slopes in the range $0.050 \leq b_T \leq 0.060$ V decade^{-1}, in agreement with previously reported data [9] (Fig. 2).

3.2. Cyclic voltammetric data

3.2.1. Blank and aqueous TU-containing 0.5 M sulphuric acid

Voltammograms of copper in both aqueous-free and 0.5 mM TU + 0.5 M sulphuric acid were run at 0.05 V s^{-1} from $E = -0.65$ to $E \approx 0.04$ V. For $c_{TU} = 0$ mM (Fig. 4a) the electrodissolution of copper starts at -0.06 V and increases continuously, although it exhibits a small hump at ca. -0.05 V. The reverse scan shows that the electrodeposition of dissolved copper extends from ca. 0 to -0.54 V. The cathodic current is characterised by a broad peak at ca. -0.05 V followed by a cathodic limiting current.

For 0.5 mM TU, a complex voltammogram is obtained (Fig. 4b). It shows the anodic current peak I_a and hump II_a preceding copper electrodissolution, whereas the reverse scan shows three cathodic current peaks I_c, II_c and III_c. As described elsewhere [27], peak II_a corresponds to the formation of soluble Cu(I), which occurs simultaneously with the formation of soluble Cu(II) species, peak III_c comes from the electroreduction of these species, and finally, peak II_c is related to the electrodeposition of soluble Cu(I)–TU complexes. The pair of peaks I_a/I_c corresponds to the redox reaction involving TU and FDS in solution. In

this case, the TU/FDS redox system appears in the same potential range as that found for platinum and gold in the same solution [27]. This conclusion is also supported by comparing the dependence of the open circuit potential on c_{TU} for copper, gold and platinum [27]. Finally, it should be pointed out that the main characteristics of the cyclic voltammograms do not change with v although the current peaks exhibit a linear dependence on $v^{1/2}$ [31].

3.2.2. Aqueous FDS-containing 0.5 M sulphuric acid

To determine the influence of FDS, as compared to TU, on the electrodissolution of copper, voltammograms of copper in 0.5 M sulphuric acid + 0.5 mM FDS were run, covering the potential range $-0.30 \leq E \leq 0.075$ V, i.e. where FDS is formed from TU electro-oxidation (Fig. 4). In these runs the potential routine included a potential holding at E_τ in the range $-0.100 \leq E_\tau \leq 0.075$ V for the time τ (Fig. 5a). The voltammetric scan from 0.025 V downward shows the appearance of peak II_c, which is related to the electroreduction of Cu(I) soluble species, the height of this peak increasing with τ. Voltammograms also show that the positive to negative voltammetric charge ratio (Q_a/Q_c) depends on the upper potential limit, E_u (Fig. 5b). These results indicate that the presence of FDS alone assists the formation of Cu(I) soluble species at these potentials. As E_u is moved from -0.10 to 0.075 V, the relative contribution of Cu(I) electrodissolution to the overall anodic process appears to be increased. Besides Q_a/Q_c, decreases almost linearly with E_u approaching 1 for $E_u = 0.075$ V, a figure which would correspond to the thermodynamic threshold potential for copper electrodissolution as aqueous Cu(II) ions. Therefore, for $E < 0.075$ V, TU electro-oxidation to FDS and copper electrodissolution as Cu(I)–TU complexes are the main reactions.

When similar experiments are run for $E_\tau \geq 0.01$ V (Fig. 5c), i.e. at potential values exceeding the equilibrium potential of the Cu(0)/aqueous 0.1 M Cu(II) electrode, the voltammogram shows the rapid appearance of peak III_c, which corresponds to the electroreduction of aqueous Cu(II) ions. At these positive potentials the electrodecomposition of FDS yields a dark anodic layer.

The composition of the different anodic products was investigated using different analytical techniques as described in Section 3.3.

3.2.3. TU–copper interactions at low potentials

As shown by polarisation curves at 0 V, even at the lowest c_{TU} there is a considerable hindrance of the anodic reactions. Therefore, it was interesting to investigate the lowest potential at which the coverage of the copper surface by TU could be detected. For this purpose, voltammograms of thallium upd were run covering the potential range where the alloying effect is negligible [32–35]. The blank voltammograms (Fig. 6) show the anodic and cathodic peaks of thallium upd in the potential range -0.65 to -0.45 V. The anodic to cathodic charge ratio is $Q_a/Q_c = 1$, and the process involves a charge density of 0.35 mC cm^{-2} as has been reported [34].

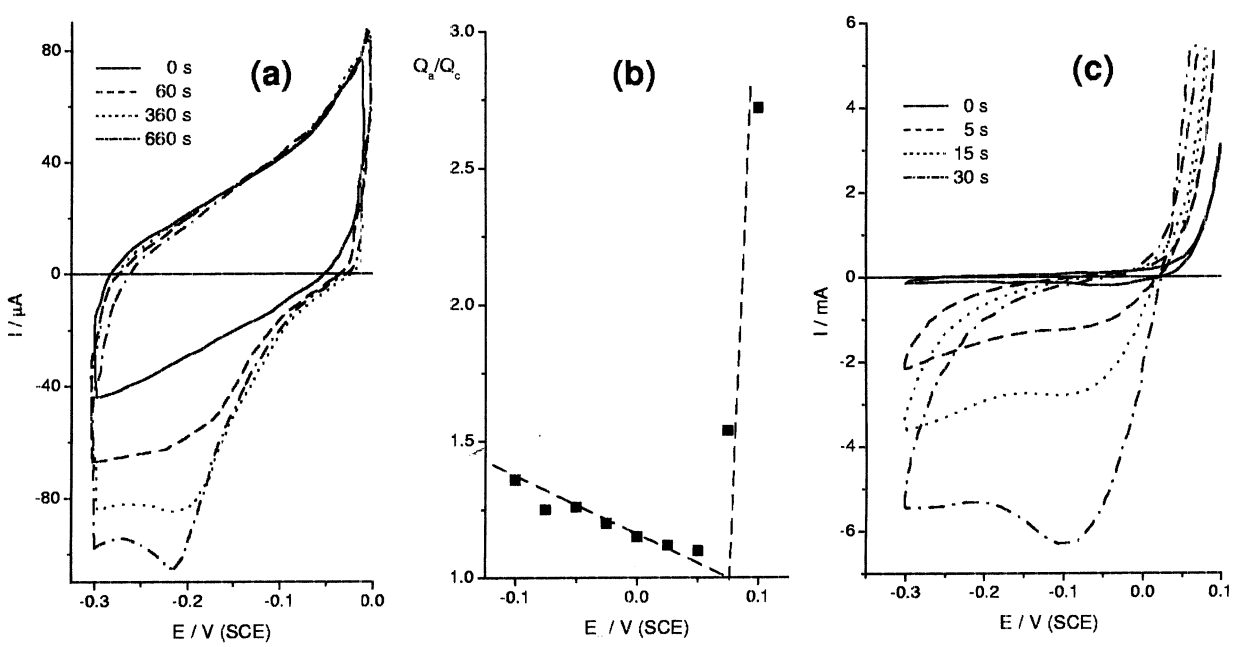

Fig. 5. (a) Single-cycle voltammograms run between 0.0 V and -0.3 V including a holding time at 0.0 V. (b) Plot of the Q_a/Q_c ratio vs. the upper potential limit (E_u) obtained from the first cycle between E_u and -0.3 V. (c) Single cycle voltammograms run between 0.1 V and -0.3 V including a holding time at 0.1 V. 0.5 mM FDS + 0.5 M sulphuric acid. $v = 0.05$ V s^{-1}. Temperature: 298 K.

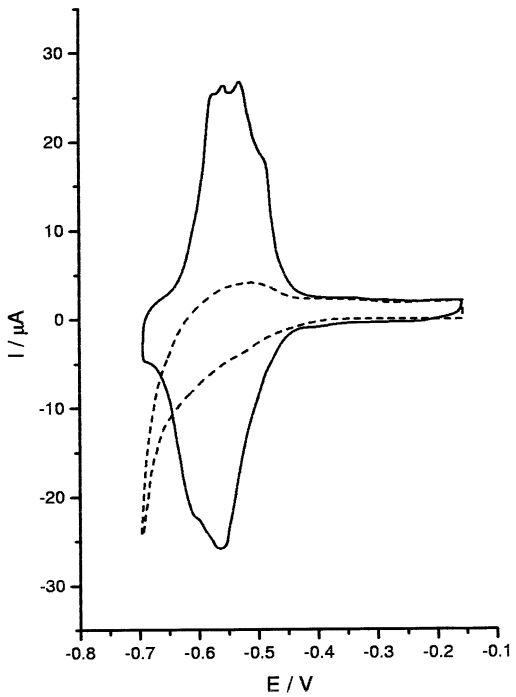

Fig. 6. Voltammograms of copper in 0.1 mM thallium sulphate + 0.5 M sulphuric acid; before (full trace) and after (dotted trace) immersion in 0.01 mM TU + 0.5 M sulphuric acid for 30 s under open circuit conditions. Electrode area 0.2 cm^2. $v = 0.05$ V s^{-1}. Temperature: 298 K.

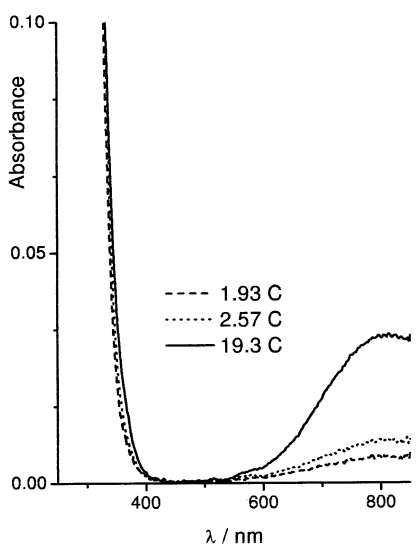

Fig. 7. Sequential absorption spectra of the electrolyte solution after different anodisation times (charge). Copper anode in 0.5 mM TU + 0.5 M sulphuric acid. The peak at 790 nm corresponds to the absorption of Cu(II) hexa-aquo ions.

The same experiment was run with a copper anode that had been previously immersed in aqueous 0.01 mM TU + 0.5 M sulphuric acid for 30 s (Fig. 6). In this case, the cyclic voltammogram shows the main contribution of the hydrogen evolution reaction (her), and a cathodic hump and a broad anodic peak, which are related to thallium upd. The thallium upd charge deconvoluted from the her is 0.12 mC cm^{-2}. Therefore, from the charge ratio of this experiment, and that from the blank, we obtain a copper surface coverage by TU of 72%. Voltammograms also show that TU–copper interaction in aqueous solutions at these potentials should be ascribed to an electroadsorption process, as recently found for gold [36].

3.3. Reaction products

For the range $-0.30 \leq E \leq 0.07$ V, products from copper anodisation in aqueous TU-containing sulphuric acid depend on c_{TU} and E.

At low c_{TU} and $E < 0.1$ V, complex **I** is produced. The UV–vis absorption spectrum for this complex in aqueous solution starts from $\lambda < 350$ nm (Fig. 7) with maximum absorption at ca. 240 nm [11]. Complex **I** was crystallised and, according to X-ray diffractometry data, it was identified as crystalline $[Cu_2(TU)_5]SO_4 \cdot 3H_2O$ [21].

After a certain electrolysis time, which depends on c_{TU} and j, a critical Cu(I)/TU molar concentration ratio at the anode is attained favouring the formation of film I. The elemental chemical analysis of film I yielded C = 10.2, H = 4.6, N = 26.7, S = 28.3 and ashes = 25.1%, which for these four elements is consistent with the formula of complex **I**, although the high content of ashes from copper in the sample prevented a more accurate stoichiometric determination. After the dissolution and recrystallisation of film I, the complex $[Cu_4(TU)_7)](SO_4)_2 \cdot H_2O$ was obtained [21].

Wide XPS spectra of film I, average thickness $\langle h \rangle \approx$ 160 nm, showed peaks corresponding to Cu, S, O and C, and Auger peaks of Cu and O (Fig. 8). Narrow high

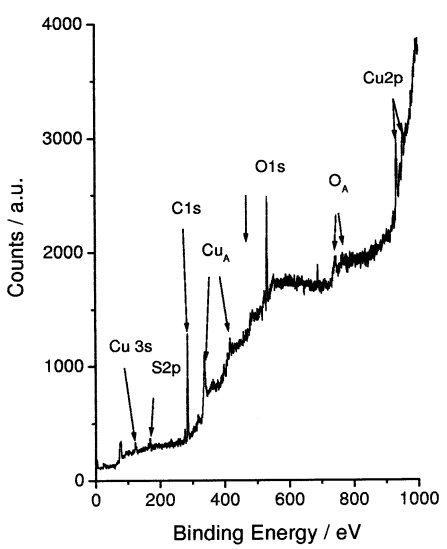

Fig. 8. Wide XPS spectrum of the anodic film formed on copper in 0.5 mM TU + 0.5 M sulphuric acid at $E = 0.06$ V for $t = 7200$ s.

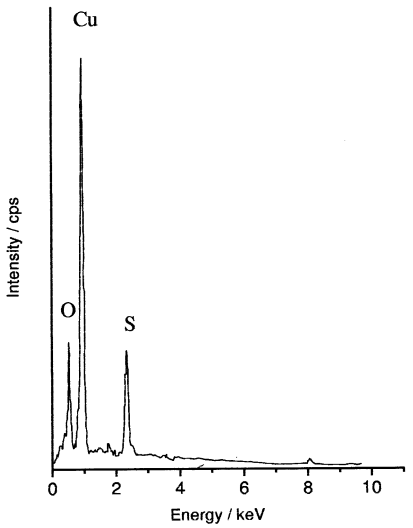

Fig. 9. EDAX spectrum of the anodic film formed on copper in 0.5 mM TU + 0.5 M sulphuric acid at 0.1 V for 8100 s.

resolution spectra for the levels C1s, N1s, O1s, Cu2p and S2p were recorded before and after sputtering the sample surface with Ar^+ for 120 s leaving a small fraction of the initial film, $\langle h \rangle \approx 14$ nm. In both cases, the spectra confirmed the presence of Cu, O, S and N. It should be noted that film I could not be produced on copper in aqueous TU-free sulphuric acid on platinum in aqueous TU-containing solution by anodic polarisation.

At low E and large c_{TU}, soluble complex **III** is obtained. Complex **III** has also been recrystallised and identified as $[Cu_2(TU)_6]SO_4 \cdot H_2O$ [21].

For $E \approx 0.07$ V, after a sufficiently long electrolysis to decrease the concentration of TU in the solution, the formation of the Cu(I)–TU complex from Cu(I) and FDS takes place. Finally, for $E > 0.07$ V, FDS at the reaction interface is exhausted and aqueous Cu(II) ions are formed (Fig. 5c). The UV–vis absorption spectra of the solution then exhibit a peak at 790 nm [37] related to hexa-aquo Cu(II) ions, the height of the absorption peak increasing with the anodisation time (Fig. 7).

For $E \geq 0.075$ V, the above mentioned reactions are accompanied by the electrodecomposition of FDS and a change in the composition of the anodic film. For $c_{TU} > c_{TU,c}$ and $E \approx 0.075$ V, film I turns from grey–white to brown resulting in a new type of film. For $E > 0.075$ V, as c_{TU} is diminished, the anodic film turns into a blackish sludge (film II).

The average composition of film II was determined by EDAX and XPS, although the interpretation of data is somewhat obscure due to the resulting patched structure of the film after drying. Average EDAX data showed that the film contains Cu = 66.8, S = 18.6 and O = 15.1% (Fig. 9). EDAX failed for nitrogen detection. However, data from the top of the patches indicate the formation of sulphur-containing species (S = 24%) with an excess of copper (Cu = 76%). Thus, film II can be interpreted as being made of either Cu_2S or a mixture of CuS + Cu. The presence of these products implies the electrodecomposition of FDS to S atoms or CN residues [38] on copper yielding copper sulphide as the main residue [39]. In this case, the excess of copper might be due to the penetration of the EDAX signal into bulk copper.

3.4. Complementary coulometric data

To confirm the stage at which TU and FDS depletion takes place and Cu(II) ions are produced, coulometric experiments using aqueous 0.5 mM TU and 10 mM TU in 0.5 M sulphuric acid were made. In the former solution, aqueous Cu(II) ions were detected spectrophotometrically when the charge passed exceeded $Q_a \approx 0.05$ C, whereas for the latter, there was no spectrophotometric evidence of cupric species up to $Q_a \approx 10$ C.

4. Discussion

4.1. Adsorption and electroadsorption of TU on copper

The adsorption of TU during electrolytically driven metal lattice formation and dissolution is difficult to observe, particularly under conditions far from equilibrium. As has been demonstrated in 1 M $HClO_4$ by radiotracer measurements [40], TU adsorption on copper from aqueous acid solutions reaches a maximum at ca. 0.34 V. Furthermore, radiotracer and electroreflectance data obtained for copper in aqueous 1.5 M sulphuric acid and $c_{TU} < 1$ mM have shown that the adsorption of TU approaches the monolayer as the potential is increased to 0.27 V, whereas for $c_{TU} > 1$ mM, TU adsorption increases sharply up to multilayers [16]. SERS [41] and electroreflectance [16] data indicate that TU adsorption occurs on copper via the sulphur atom. This is consistent with a $3d^{10}4s$ electronic structure for the copper atom in the metal phase with the binding to S atom from TU, almost entirely due to the 4s electron [42], either for the C=S or the C–SH tautomeric form of the TU molecule [43,44].

In the potential range -0.65 to -0.45 V, the ratio of thallium upd charge in the presence and in the absence of TU on copper is 0.28. These results indicate that TU adsorbates are already produced in this low potential range by an electroadsorption reaction such as [45]

$$Cu + TU \rightarrow [Cu(TU^*)_{ad}]^{\delta+} + H^+ + (\delta + 1)e^- \quad (1)$$

yielding a fractional monolayer coverage by TU*, where TU* stands for a deprotonated TU molecule.

Therefore, the initial copper electrode surface, for $j \to 0$, should be considered as already covered to a great extent by TU adsorbates. In this case, the adsorbate structure is probably comparable to that of TU on gold [36] at the same pH and potential range. Reaction (1) occurs in the same potential range where the electroadsorption of thiols takes place [44].

As recently discovered for Au(111)–TU adsorption interactions [36], by conveniently adjusting the applied potential between -1.0 and 0 V (versus SCE), different adsorbate lattices can be produced. In situ STM images showed TU adsorbates with different packing, adsorbed FDS, and various arrangements of adsorbed sulphur atoms. In principle, the similarity of voltammograms for platinum, gold and copper [27] suggests that the type of adsorbates described for gold or something like may also exist for copper in contact with TU-containing solutions.

On the other hand, besides the copper–TU interactions described above, the interaction of SO_4^{2-} and HSO_4^- with a copper electrode in the absence of TU in the solution has been concluded from SERS spectra [41]. The enhancement of the frequency corresponding to the SO_4^{2-} species in TU–sulphate-containing solutions, is consistent with the coadsorption of SO_4^{2-} and HSO_4^- together with TU at the copper electrode. The shift of the corresponding bands in the presence of TU suggests a complex formation [41]. This is consistent with the type of products found in the range $-0.3 \le E \le 0$ V.

4.2. Reaction pathway of copper electrodissolution as Cu(I) in aqueous TU-containing 0.5 M sulphuric acid

In general, copper electrodissolution shows an increasing polarisation due to the presence of adsorbates. For $E < E_b$ at low c_{TU}, the surface coverage by these adsorbates increases with c_{TU}. A similar inhibition of copper electrodissolution caused by 5-mercapto-1-phenyltetrazole adsorption at the monolayer or submonolayer level has been reported recently [46]. For those conditions of E and c_{TU}, the polarisation curve is mainly related to the electro-oxidation of TU to FDS in solution according to the reaction

$$2TU \to FDS + 2H^+ + 2e^- \quad (2)$$

accompanied by the electrodissolution of copper to Cu(I) species.

The rate of reaction (2) depends linearly on c_{TU} and involves the formation of the radical ion in solution $[TU]^{\bullet +}$ as a product from TU electro-oxidation [47]. At $E = -0.1$ V, it attains a mass transport limiting current, as has also been observed for platinum [28] and gold [27]. For copper, the voltammetric features of the TU/FDS redox couple are almost similar to those found for platinum and gold under comparable conditions [27].

As has been concluded earlier [10–14], in the range $-0.1 \le E \le -0.075$ V, reaction (1) favours the electrodissolution of copper to Cu(I), according to a reaction such as

$$[Cu(TU^*)_{ad}]^{\delta +} \rightleftharpoons [Cu(TU)]^+_{aq} + (1-\delta)e^- \quad (3)$$

Reaction (3) is accompanied by the formation of FDS that assists the electrodissolution of copper through the formation of either a surface reaction intermediate such as $Cu(FDS)_{ad}$ or by the radical ion $TU^{\bullet +}$ in solution [47]. These reactions can be written as follows

$$\{Cu\}Cu(TU^*)_{ad} + TU_{sol} \to \{Cu\}[Cu(FDS)]_{ad} + H^+ + e^- \quad (4a)$$

$$\{Cu\}[Cu(FDS)]_{ad} \to [Cu(TU)]^+_{sol} + \{Cu\}Cu(TU^*)_{ad} + e^- \quad (4b)$$

$$\{Cu\}[Cu(FDS)]_{ad} + H^+ \to Cu(TU^*)_{ad} + (TU)^{\bullet +}_{sol} \quad (4c)$$

$$2(TU)^{\bullet +}_{sol} \to FDS_{sol} \quad (4d)$$

where {Cu} indicates the copper substrate, $Cu(TU^*)_{ad}$ can be considered as a precursor of copper electrodissolution, and $[Cu(FDS)]_{ad}$ reacts in two different ways as shown by reactions (4b and c); ad and sol stand for adsorbates on the copper substrate and dissolved species, respectively. The $[Cu(TU)]^+_{sol}$ species can be electroreduced to Cu(0) in the potential range of peak II_c (Fig. 4b) via the reaction

$$2[Cu(TU)]^+_{sol} + 2e^- \to 2Cu(0) + 2TU \quad (5)$$

It should be noted that the formation of a FDS adsorbate has been observed on Au(111) by in situ STM imaging [36], although the interaction of FDS with metal surfaces is expected to be weaker than that of TU, as has been earlier concluded from the comparative adsorption of thiols and disulphides on gold [48,49].

The $[Cu(TU)]^+_{sol}$ species can be considered as the building blocks for Cu(I)–TU complex formation. Thus, for $c_{TU} > c_{TU,c}$, in the potential range $-0.30 \le E \le 0.07$ V, the primary complex participates in parallel reactions with TU in the solution yielding complex ions with different stoichiometries, depending on the local concentration of TU, such as the formation of film I as a polymer-like Cu(I)–TU–sulphate complex

$$4[Cu(TU)_{ad}]^+ + 3TU + 2SO_4^{2-} \to \{[Cu_4(TU)_7]^{4+} + 2SO_4^{2-}\}_{film\ I} \quad (6)$$

and soluble complex **I**

$$2[Cu(TU)_{ad}]^+ + 3TU_{sol} \to [Cu_2(TU)_5]^{2+}_{sol} \quad (7)$$

Film I can also produce $[TU]^{\bullet +}$ radical ions in solution [27,47]. The presence of this film adds a resistance to the diffusion of the reactant towards the copper | film I interface, the reactant being either TU diffusing in-

wards from the solution or the outward migration and diffusion of $[Cu(TU)]^+$ ions to attain ligand saturation at the outer film I | solution interface. In any case, the presence of film I makes the overall anodic reaction sluggish favouring a partial replenishing of TU at the reaction interface, and assisting the formation of complex **III** either from the reaction

$$2[Cu(TU)^*_{ad}]^+ + 4TU_{sol} \rightarrow [Cu_2(TU)_6]^{2+}_{sol} \quad (8)$$

or by chemical dissolution of film I,

$$[Cu_4(TU)_7]^{4+} + 5TU_{sol} \rightarrow 2[Cu_2(TU)_6]^{2+}_{sol} \quad (9)$$

as has been recently proved [21].

Seemingly, reaction (9) occurs preferentially at the outer part of film I. The stability of both the precursor and primary complex depends on the presence of TU at the copper anode. It should be noted that the faradaic yield of reaction (6) is much lower than those of reactions (7) and (8) [24].

The reaction pathway proposed in this work is, therefore, consistent with the fact that at relatively high concentrations of TU, the electrodissolution of copper in aqueous sulphuric acid occurs as Cu(I) ions, as has been demonstrated by quartz crystal microbalance experiments [22]. It has been concluded that this process, at low current density, is rate-controlled by the diffusion of TU from the solution.

4.3. Anodic reactions for $E > 0.075$ V

For $E > 0.075$ V, the simultaneous electrodecomposition of FDS and Cu(I)–TU complexes, and the electrodissolution of copper to aqueous Cu(II) ions take place. The electrodecomposition reactions yield film II consisting of a heterogeneous residue of copper sulphides, copper and presumably $(CN)_{ad}$ species. As these reactions come to an end, the average thickness of film II practically becomes constant. Then, the reaction

$$Cu \rightarrow Cu(II)_{aq} + 2e^- \quad (10)$$

through film II takes place. The polarisation curve related to reaction (10) in the presence of film II fits a Tafel line with b_T in the range $0.050 \leq b_T \leq 0.060$ V decade^{-1} (Fig. 1).

Reaction (10) occurs through the formation of Cu(I) soluble species at the reaction interface accompanied by Cu(I) disproportionation into Cu(II) and Cu(0), as has been extensively discussed [26].

Solid products from electrodecomposition reactions as well as the presence of Cu(II) in solution are in qualitative and quantitative agreement with the XPS data.

For $c_{TU} > c_{TU,c}$, the passivity range extends from 0.04 V upwards, and passivity breakdown is observed in the neighbourhood of E_b, which in turn depends on c_{TU}. The partial rupture of the anodic film leads to localised corrosion of copper with the formation of etched pits [24].

Copper corrosion in the presence of film II becomes very similar to that found for the electro-oxidation of copper in sodium sulphide-containing solution [29,50,51]. In this case, a complex copper sulphide layer is formed at potentials slightly above the reversible Cu/Cu_2S electrode potential through a reaction similar to the chemical sulphidisation of copper [51]. This copper sulphide layer has been described as a non-stoichiometric layer approaching the stoichiometry of Cu_2S at the inner layer, and that of CuS at the outer layer. In the presence of sulphide [29,50,51], as the potential is further increased, the rupture of the copper sulphide layer also leads to the localised corrosion of copper and etched pit formation. The formation of monolayer etched pits for copper dissolution at higher potentials in aqueous 0.01 M sulphuric acid in the presence of benzotriazole has recently been reported [52].

5. Conclusions

- The anodisation of copper in aqueous low concentration TU-containing 0.5 M sulphuric acid first leads to the electro-oxidation of TU to FDS followed by the formation of $[Cu(TU)]^+$ precursor species that yield soluble Cu(I)–TU complex ions of the form $[Cu_2TU_5]^{2+}$ and $[Cu_2TU_6]^{2+}$. These reactions involve the participation of adsorbed TU species. In agreement with earlier studies, the global electro-oxidation reaction TU → FDS in solution follows intermediate kinetics governed by TU diffusion from the solution towards the copper surface, the electrochemical processes being influenced by the electroadsorption of TU and the presence of FDS in the solution.
- Cu(I) complexes are also formed anodically from FDS. The electrochemical characteristics of these complexes resemble those of Cu(I)–TU complexes.
- Under a certain critical copper ion/TU molar concentration ratio and $E < 0.075$ V, an insoluble Cu(I)–TU film is formed. This film can be dissolved with an excess of TU and recrystallised as $[Cu_2TU_6]SO_4 \cdot H_2O$.
- For $E > 0.075$ V, a heterogenous anodic film consisting of products resulting from the electrochemical decomposition of TU and FDS, is produced.
- For $E > 0.075$ V, copper electrodissolution as Cu(II) species through the heterogeneous anodic film is observed.
- Below the critical copper ion/TU molar concentration range and $E < E_b$, the polarisation curve involves a Tafel slope increasing, due to adsorbates and anodic film formation, from 0.030 V decade^{-1} for $c_{TU} = 0$ to about 0.060 V decade^{-1} for $c_{TU} \rightarrow c_{TU,c}$.

Acknowledgements

This work was financially supported by the Consejo Nacional de Investigaciones Científicas y Técnicas (CONICET) (PIP 4376) and Agencia Nacional de Promoción Científica y Tecnológica (PICT 98 06-03251) of Argentina and the Comisión de Investigaciones Científicas de la Provincia de Buenos Aires (CIC). A.S.M.A.H. thanks the Third World Academy of Science (TWAS) and CONICET for the fellowship granted.

References

[1] T.P. Hoar, Pittsburgh International Conference on Surface Reactions, The Corrosion Publishing Company, Pittsburgh, PA, 1948.
[2] T.P. Hoar, R.D. Holliday, J. Appl. Chem. 3 (1953) 502.
[3] A.C. Makrides, N. Hackerman, Ind. Eng. Chem. 47 (1955) 1773.
[4] M.J. Jannssen, Spectrochim. Acta 17 (1961) 474.
[5] T.K. Ross, D.H. Jones, J. Appl. Chem. 12 (1962) 314.
[6] K.C. Pillai, R. Narayan, J. Electrochem. Soc. 125 (1978) 1393.
[7] B.G. Ateya, B.E. El-Anadouli, F.M. El-Nizamy, Corros. Sci. 24 (1984) 497.
[8] R. Agarwal, T.K.G. Namboodhiri, Corros. Sci. 30 (1990) 37.
[9] Z.D. Stankovic, M. Vukovic, Electrochim. Acta 41 (1996) 2529.
[10] H.M. Ratajczak, L. Pajdowski, Inorg. Nucl. Chem. 36 (1974) 431.
[11] P. Javet, H.E. Hintermann, Electrochim. Acta 14 (1969) 527.
[12] F.A. Cotton, G. Wilkinson, Advanced Inorganic Chemistry, fourth ed., Wiley, Chichester, UK, 1980.
[13] E.I. Onstott, H.A. Laitinen, J. Am. Chem. Soc. 72 (1950) 4724.
[14] A. Szymaszek, J. Biernat, L. Pajdowski, Electrochim. Acta 22 (1977) 359.
[15] E.E. Farndon, F.C. Walsh, S.A. Campbell, J. Appl. Electrochem. 25 (1995) 574.
[16] G.V. Korshin, A. Petukhov, A.M. Kuznetsov, Y.M. Vyzhimov, Elektrohimiya 27 (1991) 275.
[17] F. Hanic, E. Durcanská, Inorg. Chim. Acta 3 (1969) 293.
[18] E.H. Griffith, G.W. Hunt, E.L. Amma, J. Chem. Soc., Chem. Commun. (1976) 432.
[19] E.A.H. Griffith, G.A. Spofford, E.L. Amma, Inorg. Chem. 17 (1978) 1913.
[20] M.B. Ferrari, G.F. Gasparri, Cryst. Struct. 5 (1976) 935.
[21] O. Piro, R.C.V. Piatti, A.E. Bolzán, R.C. Salvarezza, A.J. Arvia, Acta Crystallogr., Sect. B (in press).
[22] M. Alodan, W. Smyrl, Electrochim. Acta 44 (1998) 299.
[23] W.A. Spofford, E.L. Amma, Acta Crystallogr., Sect. B 26 (1970) 1474.
[24] A.S.M.A. Haseeb, P.L. Schilardi, R.C.V. Piatti, A.E. Bolzán, R.C. Salvarezza, A.J. Arvia, J. Electroanal. Chem. 500 (2001) 543.
[25] P. Shigolev, Electrolytic and Chemical Polishing of Metals, Freund, Tel Aviv, 1974.
[26] D.K.Y. Wong, B.A.W. Coller, D.R. MacFarlane, Electrochim. Acta 38 (1993) 2121.
[27] A.E. Bolzán, R.C.V. Piatti, R.C. Salvarezza, A.J. Arvia, Extended Abstracts, 50th ISE Meeting, Pavia, Italy, 1999.
[28] A.E. Bolzán, I.B. Wakenge, R.C. Salvarezza, A.J. Arvia, J. Electroanal. Chem. 475 (1999) 181.
[29] D. Vázquez Moll, M.R.G. de Chialvo, R.C. Salvarezza, A.J. Arvia, Electrochim. Acta 30 (1985) 1011.
[30] U. Bertocci, D.R. Turner, in: A.J. Bard (Ed.), Encyclopedia of Electrochemistry of the Elements, vol. II, Marcel Dekker, New York, 1974 (Chapter VI).
[31] A.E. Bolzán, I.B. Wakenge, R.C.V. Piatti, R.C. Salvarezza, A.J. Arvia, submitted.
[32] D.M. Kolb, in: H. Gerischer, G. Tobias (Eds.), Advances in Electrochemistry and Electrochemical Engineering, vol. 11, Wiley, New York, 1978.
[33] R.R. Adzic, Israel J. Chem. 18 (1979) 166.
[34] D.A. Berg, D.S. Nadezdhim, R.G. Barradas, J. Electroanal. Chem. 355 (1993) 165.
[35] A. Hernández Creus, R.M. Souto, S. González, M.M. Laz, R.C. Salvarezza, A.J. Arvia, Appl. Surf. Sci. 81 (1994) 387.
[36] O. Azzaroni, B. Blum, R.C. Salvarezza, A.J. Arvia, J. Phys. Chem. Lett. B 104 (2000) 1395.
[37] M.H. Jaffé, M. Orchin, Theory and Application of Ultraviolet Spectroscopy, Wiley, New York, 1965.
[38] M. Yan, K. Liu, Z. Jiang, J. Electroanal. Chem. 408 (1996) 225.
[39] J. Hrbek, J. de la Figuera, K. Pohl, T. Jirsak, J.A. Rodríguez, A.K. Schmidt, N.C. Bartelt, R.Q. Hwang, J. Phys. Chem. B 103 (1999) 10557.
[40] G. Horanyi, E.M. Rizmayer, P. Joó, J. Electroanal. Chem. 149 (1983) 221.
[41] G.M. Brown, G.A. Hope, D.P. Schweinsberg, P.M. Fredericks, J. Electroanal. Chem. 380 (1995) 161.
[42] L. Pauling, The Nature of the Chemical Bond, Cornell University Press, New York, 1960.
[43] M. Fleischmann, I.R. Hill, G. Sundholm, J. Electroanal. Chem. 157 (1983) 359.
[44] C.A. Widrig, C. Chung, M.D. Porter, J. Electroanal. Chem. 310 (1991) 335.
[45] D.W. Hatchett, K.J. Stevenson, W.B. Lacy, J.M. Harris, H.S. White, J. Am. Chem. Soc. 119 (1997) 6596.
[46] E. Szöcs, G. Vastaj, A. Shaban, G. Konczos, E. Kálmán, J. Appl. Electrochem. 29 (1999) 1339.
[47] S.J.J. Reddy, V.N. Krishnan, J. Electroanal. Chem. 27 (1970) 473.
[48] L.-H. Wan, Y. Hara, H. Noda, M. Osawa, J. Phys. Chem. B 102 (1998) 5943.
[49] T.Y. Leung, M.C. Gerstenberg, D.J. Lavrich, G. Scoles, F. Schreiber, G.E. Porter, Langmuir 16 (2000) 549.
[50] T.P. Hoar, A.J.P. Tucker, J. Inst. Metals 81 (1952) 665.
[51] E.M. Kahiry, N.A. Darwish, Corros. Sci. 13 (1973) 141.
[52] W. Polewska, M.R. Vogt, O.M. Magnussen, R.J. Behm, J. Phys. Chem. B 103 (1999) 10440.